frontiers in Marine Science

ORIGINAL RESEARCH
published: 30 June 2016
doi: 10.3389/fmars.2016.00109

P- and N-Depletion Trigger Similar Cellular Responses to Promote Senescence in Eukaryotic Phytoplankton

Sebastian D. Rokitta[1]*, *Peter von Dassow*[2, 3, 4], *Björn Rost*[1] and *Uwe John*[1]

[1] Marine Biogeosciences, Alfred Wegener Institute, Helmholtz Centre for Polar and Marine Research, Bremerhaven, Germany, [2] Facultad de Ciencias Biológicas, Pontificia Universidad Católica de Chile, Santiago, Chile, [3] Instituto Milenio de Oceanografía de Chile, Concepción, Chile, [4] Centre National de la Recherche Scientifique, Station Biologique de Roscoff, UPMC, Sorbonne Universités UMI3614, Roscoff, France

Global change will affect multiple physico-chemical parameters of the oceans, amongst them also the abundances of macronutrients like phosphorus and nitrogen that are critical for phytoplankton growth. Here, we assessed the transcriptomic responses to phosphorus (P) depletion in the haploid and diploid life-cycle stage of the coccolithophore *Emiliania huxleyi* (RCC1217/1216) and compared the results with an existing dataset on nitrogen (N) depletion. The responses to the two depletion scenarios within one particular life-cycle stage were more similar at the transcriptome level than the responses of the two stages toward only one particular depletion scenario, emphasizing the tripartite nature of the coccolithophore genome. When cells senesced in both scenarios, they applied functionally similar programs to shut down cell-cycling, re-adjust biochemical pathways, and increase metabolic turnover to efficiently recycle elements. Those genes that exclusively responded to either P- or N-depletion modulated the general response to enhance scavenging, uptake, and attempted storage of the limiting nutrient. The metabolic adjustments during senescence involved conserved and ancient pathways (e.g., proline oxidation or the glycolytic bypass) that prolong survival on the one hand, but on the other hand give rise to toxic messengers (e.g., reactive oxygen species or methylglyoxal). Continued senescence thus promotes various processes that lead to cell death, which can be delayed only for a limited time. As a consequence, the interplay of the involved processes determines how long cells can endure severe nutrient depletion before they lyse and provide their constituent nutrients to the more viable competitors in their environment. These responses to nutrient depletion are observable in other phytoplankton, but it appears that *E. huxleyi*'s outstanding endurance under nutrient deficiency is due to its versatile high-affinity uptake systems and an efficient, NAD-independent malate oxidation that is absent from most other taxa.

Keywords: *Emiliania huxleyi*, transcriptomics, phosphorus, nitrogen, nutrient depletion, cell death, proline oxidase, autophagy

OPEN ACCESS

Edited by:
Karla B. Heidelberg, University of Southern California, USA

Reviewed by:
Gerhard J. Josef Herndl, University of Vienna, Austria
Kevin John Flynn, Swansea University, UK

***Correspondence:**
Sebastian D. Rokitta
sebastian.rokitta@awi.de

Specialty section:
This article was submitted to Aquatic Microbiology, a section of the journal Frontiers in Marine Science

Received: *05 February 2016*
Accepted: *10 June 2016*
Published: *30 June 2016*

Citation:
Rokitta SD, von Dassow P, Rost B and John U (2016) P- and N-Depletion Trigger Similar Cellular Responses to Promote Senescence in Eukaryotic Phytoplankton. Front. Mar. Sci. 3:109. doi: 10.3389/fmars.2016.00109

INTRODUCTION

Planktonic primary producers form the basis of the marine food webs and drive the biogeochemical cycles of elements in the oceans (Field et al., 1998). Understanding the subcellular functioning of these cells is a basic and important quest in biological research, and a prerequisite for depicting their behavior in models to simulate their reactions to a changing environment. Global change will affect multiple physical and chemical parameters of the oceans, e.g., temperature, pH, and also the abundances of macronutrients like phosphorus (P) and nitrogen (N) that are critical for growth. In open ocean regions, elevated atmospheric temperatures will lead to enhanced stratification, thereby restricting nutrient input from depth into euphotic surface waters (Rost and Riebesell, 2004; Steinacher et al., 2010; Doney et al., 2012). For coastal waters, in turn, it is anticipated that altered wind systems may strengthen eastern boundary upwelling, and thus enhance primary productivity (Bakun et al., 2010). These alterations are expected to affect phytoplankton community composition, ecosystem functioning, and ultimately also biogeochemical cycles.

The globally significant coccolithophore *Emiliania huxleyi* is an especially interesting model organism for understanding adaptations to changes in nutrient abundances. The calcifying stage of this microalgae serves a complex role in biogeochemistry, because its photosynthesis contributes to the 'organic carbon pump,' and at the same time, its calcification contributes to the 'inorganic carbon pump' (Rost and Riebesell, 2004). In addition, the ballasting of organic aggregates by the heavy calcite material enhances subsequent depth export of organic aggregates (Klaas and Archer, 2002), giving coccolithophores a critical role in the regulation of the oceans' biological carbon pumps. *E. huxleyi* is also one of the most successful microalgae in contemporary oceans; it has a global distribution from the tropics to the polar fronts (Mohan et al., 2008), is regularly found in phytoplankton assemblages and is able to form large monospecific blooms (Tyrrell and Merico, 2004). It is highly competitive in strongly stratified 'high light/low nutrient regimes,' due to its high-light tolerant photosynthetic machinery (Tyrrell and Merico, 2004; Löbl et al., 2010; Mckew et al., 2013) and efficient cellular N management (Rokitta et al., 2014; McKew et al., 2015). Furthermore, *E. huxleyi* has been shown to possess effective P-uptake systems, involving an external alkaline phosphatase that's affinity ranks amongst the highest ever reported (Riegman et al., 2000). As a consequence, blooms of this species have been often attributed to 'higher-than-Redfield' NO_3^-:PO_4^{3-} ratios in the seawater (Paasche, 2002; Tyrrell and Merico, 2004), i.e., when there is an undersupply of P relative to N, although this alone does not necessarily imply a situation of physiological limitation, e.g., of growth. However, a review by Lessard et al. (2005) concluded from observational evidence that *E. huxleyi* blooms are more generally associated with low inorganic nutrient levels, and not specifically conditions of low nutrients with high N:P ratios. Thus, the mechanisms that ensure *Emiliana*'s survival (and often dominance) under nutrient-limiting conditions are still not fully resolved.

E. huxleyi has a heteromorphic haplo-diplontic life-cycle, alternating between a calcified non-motile diploid (2N) cell and a non-calcified motile haploid (1N) cell (Green et al., 1996; Von Dassow et al., 2009). It thereby also provides a unique system in which the consequences and benefits of haploidy can be studied, especially with respect to genome usage and the biochemical constraints underlying the responses to environmental parameters. Furthermore, the heteromorphic life-cycle facilitates comparative studies on physiology, as the two cell types show major functional differences but have the same genome. Besides its postulated function as an ecological strategy to escape viral infection (Frada et al., 2008), it has been hypothesized that haploid microorganisms in general, having only half the genomic P-demand, could have evolutionary advantages in oligotrophic regimes or post-bloom scenarios (Lewis, 1985). Such a mechanism may have contributed to the manifestation and retention of a haplo-diplontic life-cycle strategy in *E. huxleyi* (Von Dassow et al., 2009).

The availability of multiple genomic (Read et al., 2013; Von Dassow et al., 2015) and transcriptomic resources (Wahlund et al., 2004; Von Dassow et al., 2009; Rokitta et al., 2011, 2012; Kegel et al., 2013; Keeling et al., 2014) for *E. huxleyi* facilitate the application of 'omics' approaches to deepen physiological studies, leading to an emerging (and also converging) picture of how eukaryotic phytoplankton cells behave under changing environments, especially under nutrient depletion. As much of the modern ocean is limited by the availability of inorganic N, we earlier conducted transcriptome screenings with haploid and diploid *E. huxleyi* to assess the responses to N-depletion (Rokitta et al., 2014). We could identify the molecular machinery that is regulated by the cell to decrease protein biosynthesis and organelle activity, and that eventually facilitates the transition to senescence. In this context, both life-cycle stages restructured the ornithine-urea-cycle, similar to what has been reported in diatoms (Allen et al., 2011), likely supporting the efficient budgeting of N under limiting conditions. Proline oxidase (POX) was strongly induced under N-depletion. This enzyme catalyzes the mitochondrial oxidation of proline (Phang et al., 2012), so that its reductant input to the electron transfer chain should scale with the re-routing of cellular N into the associated biochemical pathways (which were also restructured when the cell-cycling was arrested). Consequently, it was interpreted to function as a 'redox-sensor' that monitors cellular N stocks and ultimately stops cell proliferation (Rokitta et al., 2014). The involvement of POX in the regulation of growth-arrest vs. proliferation has been impressively demonstrated in the context of cancer research (Liu et al., 2009; Phang et al., 2012). Under N-depletion, both life-cycle stages of *E. huxleyi* also strongly induced a malate:quinone-oxidoreductase (MQO), an enzyme that efficiently circumvents respiratory complex I by facilitating reductant input into the electron transfer chain, without the need for N-rich NAD, and under adverse cellular redox states (Molenaar et al., 1998; Kather et al., 2000; Rokitta et al., 2014).

Here, we present data from an experiment in which the cells were exposed to P-depletion in the external media. We assessed the transcriptomic response by means of microarrays, and analyzed the functional overlap with the N-depletion response

acquired earlier (Rokitta et al., 2014) as well as the peculiarities of the exclusive responses to N- and P-depletion. Thereby, we could extract the general genetic response that facilitates the arrest of cell-cycling under any of the depletion scenarios, and also the specific responses that are exclusively triggered under the particular depletion scenarios.

METHODS

Culturing, Growth, and Fluorometry

Cells of *E. huxleyi* strains RCC1216 (diploid, isolated from the Tasman Sea) and RCC1217 (the haploid sub-strain originating from RCC1216) were obtained from the Roscoff culture collection and cultured in 5L Schott bottles (biological triplicates). Cultures were grown at 15°C under a light:dark cycle of 16:8 h with irradiances of 250 ± 25 μmol photons m^{-2} s^{-1} (in the middle of the culture vessel; FQ 54W/965HO daylight lamps; OSRAM, Munich, Germany), confirmed with a datalogger (LI-1400; Li-Cor, Lincoln, NE, USA) equipped with a 4π-sensor (Walz, Effeltrich, Germany). Culture medium was prepared with aged, 0.2 μm filtered North Sea seawater (salinity 32). The nutrient-replete control medium was enriched with vitamins and trace-metals according to the F/2 recipe, (Guillard and Ryther, 1962), as well as with 100 μmol L^{-1} nitrate (NO_3^-) and 5 μmol L^{-1} phosphate (PO_4^{3-}). The 'P-depleted' medium was supplemented with vitamins, trace-metals and 100 μmol L^{-1} NO_3^- only. The low inorganic nutrients naturally present in North Sea seawater and carry-over from the cultures used to inoculate experiments added an additional ∼0.5 μmol L^{-1} PO_4^{3-} and ∼8 μmol L^{-1} NO_3^-. Prior to the inoculation in experimental media, cells were acclimated to experimental conditions for at least 10 days in dilute batch, in which exponential growth of cells was maintained under nutrient-replete conditions. Over the duration of the experiment (12 days), the culture vessels were aerated with humidified room-air (flow-rate 130 ± 20 mL min^{-1}) to avoid cell sedimentation and to re-equilibrate dissolved inorganic carbon (DIC). In addition, culture bottles were manually swirled several times a day to maintain cells in suspension.

The cell concentrations were assessed daily with a Multi-Sizer III particle counter (Beckman-Coulter, Fullerton, USA) with a 100 μm aperture tube (applied current 800 μA, gain setting 4). Specific, cell-based growth rates (μ) were calculated from cell concentrations using the equation $\mu = [\ln(c_1) - \ln(c_0)]\ \Delta t^{-1}$, where c_0 and c_1 are the cell concentrations at two time points and Δt is the time interval. The optical properties of cells were examined by flow cytometry at three time points during the experiment (when all cultures were still growing exponentially, during the transition to stationary phase when the cell-based growth rate was near zero in nutrient-deplete conditions, and at the end of the experiment when all cultures were in stationary phase. Samples of 1.8 ml were fixed by adding 0.2 ml of 10% formaldehyde, 0.5% glutaraldehyde, 10 mM Na-borate pH 8.5, and measured on a FACS Calibur flow cytometer (BD Biosciences, San Jose, CA, USA) with a 488 nm laser. Measured parameters were forward and side light scatter (FSC and SSC) and red chlorophyll fluorescence. All parameters were normalized to values of 2 μm YG FlowCheck Alignment microspheres (Polysciences, Warrington, PA, USA) added as internal standards to each sample.

To monitor inorganic carbon chemistry over the course of the experiment, total alkalinity (TA) was inferred from linear Gran-titrations (Dickson, 1981; TitroLine alpha plus burette, Schott, Mainz, Germany). DIC was measured colorimetrically (Stoll M.H.C. et al., 2001), using a TRAACS CS800 autoanalyzer (Seal Analytical, Norderstedt, Germany). Analyses of dissolved inorganic nitrite and nitrate as well as phosphate were done according to the methods described by Strickland and Parsons (1972) which were adapted to run on a QuAAtro 39 continuous-flow autoanalyzer (Seal Analytical). To assess functionality of photosystems, the ratios of variable:maximal fluorescence (F_v/F_m) were measured using a fast-induction relaxation fluorometer (FIRe, Satlantic, Halifax, Canada).

For the determination of elemental quotas of particulate organic C, N, and P (POC, PON, POP), algal cultures were gently filtered on pre-combusted GF/F filters (12 h, 500°C, 1.2 μm pore size; Whatman, Maidstone, UK). For the determination of POC contents, filters were acidified with 200 μL 0.2 mol L^{-1} HCl (Merck) to remove calcite. POC and PON analyses were carried out on a EuroVector CHNS-O elemental analyzer (EuroEA, Milano, Italy) that was calibrated with acetanilide standards (measurement uncertainty 1.5 and 2.2 μg in N and C respectively, having sample amounts of >30 and >150 μg N and C respectively). Cellular POP quotas were assessed by colorimetric measurements of molybdenum-blue complexes that form with orthophosphate, which is liberated by the complete sulphuric acid-based oxidation of filtered cells (Strickland and Parsons, 1972). Cellular quotas of calcium (a measure of particulate inorganic carbon, i.e., calcium carbonate) were assessed from samples filtered onto polycarbonate membrane filters using the ICP-MS method developed by Stoll H.M. et al. (2001).

Microarray Hybridization

Cultures were sampled for RNA at two time points that reflect 'early depletion' (days 9 and 10 in haploid and diploid cultures, respectively, i.e., 3–4 days after the detection limit for phosphate was reached) and 'full depletion' (days 11 and 12 in haploid and diploid cultures meaning 6–7 days after detection limits for phosphate were reached). As a reference, RNA was sampled from haploid and diploid cultures grown in control medium (P- and N-replete) at days 6 and 7, reflecting unlimited exponential cell-growth in dilute culture. The transcriptome screening followed the protocol established in Rokitta et al. (2012). In brief, ∼1.5 × 10^7 cells were harvested and disrupted in a bead mill. The extracted RNA (RNeasy, Qiagen, Hilden, Germany) was DNAse treated and enriched by ultrafiltration (MicroCon YM 30 columns, Millipore, Darmstadt, Germany). Integrity of isolated RNA was verified using a Bioanalyzer 2100 (Agilent, Waldbronn, Germany). RNA Spike-In Mix (Agilent, p/n 5188–5279) was added to 250 ng RNA of the samples as a benchmark of hybridization performance prior to cDNA synthesis and cRNA synthesis/labeling reactions (Two-color low RNA Input fluorescent linear amplification kit, Agilent, p/n 5184–3523). 750 ng of each Cy-3 and Cy-5 labeled cRNA were hybridized

onto 2*105K *E. huxleyi* custom-built microarrays (Agilent, Design# 022065). Three microarray probes were designed for each of 28670 transcript clusters (i.e., on-chip technical replication). Hybridization was performed following the Two-Color Microarray-based Gene Expression Analysis protocol (Agilent, p/n 5188–5242). Arrays were immediately scanned after hybridization with a G2505C microarray scanner (Agilent) using standard photomultiplier tube settings and 5 μm scan resolution. In the microarray hybridizations, every biological replicate was hybridized against the same common control baseline (i.e., pooled control RNA from all treatments) to minimize hybridization biases. Treatment-vs.-treatment expression ratios were then calculated from the single treatment-vs.-control expression ratios. All further reported expression ratios are relative to the control, i.e., unlimited exponential growth of cells in the P-replete treatment.

Data Treatment

Raw data was extracted with Feature Extraction Software version 9.0 (Agilent). Analysis was performed using GeneSpring 11 (Agilent). LOWESS-normalized data were submitted to the MIAMExpress database hosted by the European Bioinformatics Institute (EBI; www.ebi.ac.uk/arrayexpress; accession code E-MTAB-3877). The hybridization results of the biological triplicates (i.e., treatment-vs.-treatment expression ratios) were tested for significance using multiple comparison tests (ANOVA) prior to correcting the obtained *p*-values for false discoveries (Benjamini and Hochberg, 1995). Regulation was judged significant when probe-specific corrected *p*-values were <0.05. The dataset was then reduced to only those probes which detected expression changes in response to the P-depletion treatment by more than 1.5-fold. When a divergent regulation was reported, i.e., probes for the same transcript cluster indicated regulation in opposite directions, the entire probe set was excluded from further analyses (<15 probe sets per hybridization). In the cases where only one out of three probes reported significant differential expression but two probes reported unaltered expression, the respective probe sets were also excluded from further analyses to further increase the confidence level of results (300–700 probe sets per hybridization). The remaining probe sets were then merged, and are in the following reported as significantly regulated features representing one transcript cluster. For completeness, the averaged fold-change values as well as (corrected) *p*-values are reported for every transcript cluster.

Data Annotation

Significantly regulated clusters were assigned to an annotation table. This table was generated using BLASTn similarity searches, in which the 28670 transcript clusters were aligned with the 'Emihu1_best_transcripts' database provided by the Joint Genome Institute (JGI). After excluding alignments with an e-value $>10^{-5}$, the two best aligning, but different transcript models were implemented into the annotation table. This allowed the assignment of ∼21740 investigated transcript clusters to models existing in the JGI *E. huxleyi* gene catalog. Assigned JGI model IDs were then aligned with the 'best gene-model' predictions, based on similarity to eukaryotic orthologous genes (KOG; provided by the JGI). This KOG-database harbors functional information on ∼11930 different *E. huxleyi* gene models. Additionally, generic information on the investigated transcript clusters was obtained by Blast2GO (B2G) queries (Conesa et al., 2005; *e*-value cutoff at 10^{-6}), and the GO information was augmented to the annotation. The final transcriptome screening involved ∼10.000 *E. huxleyi* transcripts with a confidently predicted function. The integrity and validity of gene models of interest that are discussed in the text were reconfirmed by model inspection in the JGI genome database and by BLAST searches. In the text, exemplary transcripts of interest are notated with their numerical cluster identifiers.

RESULTS AND DISCUSSION

Growth Characteristics and Fluorometry

During the experiment, specific cell-based growth rates, as determined from numbers of the diploid (2N) and haploid (1N) cells, started off in the range of 0.9–1.1 d^{-1} when cultures were growing under nutrient-replete conditions (**Figures 1A,B**). With the onset of P-depletion at days 6 and 7, cells stopped dividing, and the growth rates calculated from cell numbers decreased rapidly to approach zero around day 12. Nutrient analyses show that the P-depleted cultures had consumed all phosphate (PO_4^{3-}) by days 6 and 7 (**Figure 1C**), whereas the concentration of nitrate (NO_3^-) remained well above limiting levels (**Figure 1D**). This demonstrates that P-depletion, and not N-depletion caused the cells to enter stationary phase. Interestingly, after depletion of PO_4^{3-}, NO_3^- consumption was also greatly decreased. This suggests that in *E. huxleyi,* the uptake of non-limiting macronutrients (here N), is mechanistically coupled to the uptake and assimilation of the limiting nutrient (P) as also observed in other microalgae (Flynn, 2008).

As a consequence of the PO_4^{3-} depletion by days 6 and 7 in 1N and 2N cultures, respectively, the typical responses were evident from the cellular elemental quotas: The depletion of PO_4^{3-} led to significant decreases in the cellular quotas of particulate organic phosphorus (POP, **Figure 1E**), which were halved by the end of the experiment. The cellular quotas of particulate organic nitrogen (PON) were more or less unaltered (Supplemental Figure 1A). The arrested cell division caused an increase in POC quotas (**Figure 1F**), leading to greatly elevated POC:POP as well as POC:PON ratios (**Figures 1G,H**). In such small microalgae (diameter ∼5 μm), POC quotas correlate well with biomass, so that increased POC quotas also indicate an increase in cell volume, as typically observed under P-depletion (e.g., Shemi et al., 2016). In support of this, flow cytometry observations showed that FSC and SSC increased in both, 1N and 2N cultures under P-depletion (Supplemental Figures 1B,C). The high SSC in 2N cells is due to the coccoliths surrounding the cells whereas FSC is more related to cell size (Von Dassow et al., 2012). Somewhat smaller increases in these parameters were also observed before under N-limitation.

As reported by other authors (Paasche, 1998; Riegman et al., 2000), P-depletion resulted in 2N cells showing higher cellular PIC contents and PIC:POC ratios compared to replete conditions (Supplemental Figures 1D,E). However, although PIC

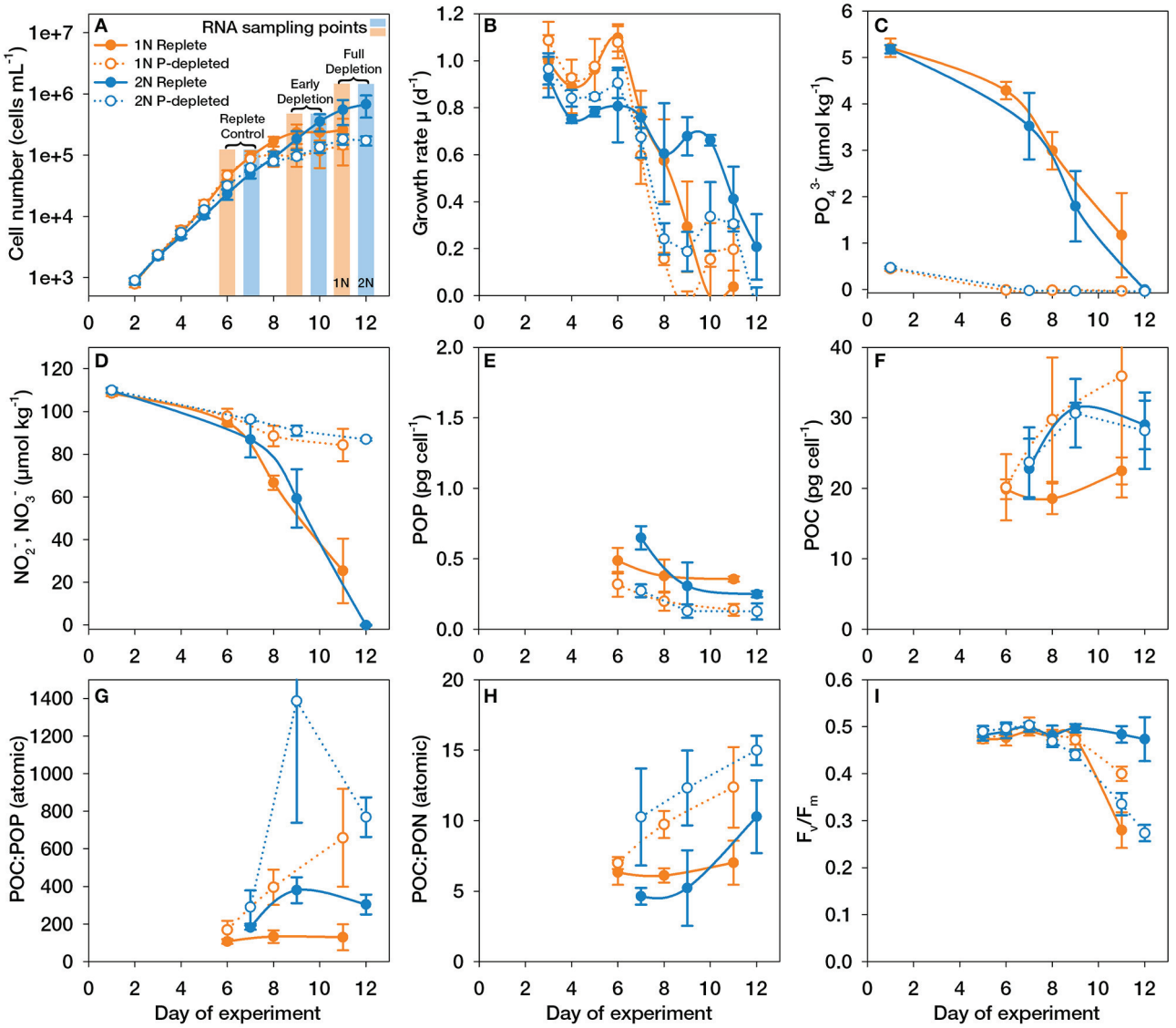

FIGURE 1 | Culture dynamics, nutrient concentrations and elemental compositions during the experiments with haploid (1N, orange) and diploid (2N, blue) *Emiliania huxleyi* grown with (P-replete, filled symbols) and without (P-depleted, open symbols) P-supplementation. (A) Cell number; **(B)** Specific growth rates; **(C)** Concentrations of phosphate (PO_4^{3-}); **(D)** Sum of concentrations of nitrite (NO_2^-) and nitrate (NO_3^-); **(E)** Quotas of particulate organic phosphorus (POP); **(F)** Quotas of particulate organic carbon (POC); **(G)** Ratio of POC:POP; **(H)** Ratio of POC:PON; **(I)** Ratios of variable:maximum fluorescence (F_v/F_m) measured over the course of the experiment; Error bars denote 1 *SD* ($n = 3$).

quotas increased over time in P-depleted cultures, the cellular PIC:POC ratios were more or less stable due to the fact that the arrest in cell division simultaneously caused increased POC quotas (Supplemental Figure 1E). Thus, we could not find direct evidence for overly increased calcification rates under P-depletion as suggested for *E. huxleyi* strain 1516 (Dyhrman et al., 2006). These elemental analyses clearly demonstrate that the cells experienced external P-depletion during the time of culture growth.

In the diploid *E. huxleyi* cultures, total alkalinity (TA) decreased over the course of culture growth (Supplemental Figure 1F) due to calcification. The parallel drop in dissolved inorganic carbon (DIC; Supplemental Figure 1G), despite a replenishment by bubbling, is due to the aforementioned consumption of TA, because this is the parameter that determines the DIC uptake capacity of seawater (Wolf-Gladrow et al., 2007). In the non-calcifying haploid cultures, TA was slightly elevated (Supplemental Figure 1F) due to the consumption of NO_3^- (Wolf-Gladrow et al., 2007). As a consequence, continuous aeration caused even slight increases in DIC toward the end of the experiment (Supplemental Figure 1G). The parameters TA and DIC were used to calculate pH and [CO_2] (Supplemental

Figures 1H,I; Pierrot et al., 2006), showing that over the duration of the cell cultivation, $[CO_2]$was at all times >20 μmol kg^{-1} (i.e., sufficiently high to rule out co-limitation with inorganic C). Thus, given the high affinities of *E. huxleyi* toward CO_2 and DIC (Rokitta and Rost, 2012), these factors could not have been limiting the photosynthetic carbon uptake over the course of the experiment.

Fluorescence data showed that in replete medium, diploid cells maintained high photosynthetic efficiency throughout the experiment ($F_v/F_m = \sim 0.5$; **Figure 1I**), likely because P and N were fully consumed only at the very last day. In contrast, in P-depleted diploid cultures, photosynthetic efficiency began to drop after day 9, 2 days after PO_4^{3-} was drawn down below the detection limit, and was halved by the end of the experiment ($F_v/F_{m;day12} = \sim 0.25$; **Figure 1I**). This is in contrast to N-depletion, where diploid *E. huxleyi* cells did not show major declines in photosystem viability at all (Löbl et al., 2010; Rokitta et al., 2014). Thus, diploid *E. huxleyi* cells appear less resistant to P-depletion than to N-depletion. In the haploid life-cycle stage, F_v/F_m values dropped after day 9, in both P-depleted as well as replete cultures (**Figure 1I**). The more rapid drop of F_v/F_m in replete haploid cultures compared to P-depleted conditions is difficult to interpret, because substantial levels of both nitrate and phosphate remained in the cultures and also changes in TA and DIC were moderate. The drop in F_v/F_m values is, however, unlikely to stem from light limitation because cell densities were not sufficient to induce significant self-shading.

The haploid cultures showed a smaller drop in F_v/F_m than diploid cultures, even after having spent at least as much time in P-depletion (PO_4^{3-} levels were undetectable at day 6 in haploid cultures). Likewise, under P-depletion, haploid cells showed a smaller drop in relative chlorophyll fluorescence per cell compared to diploid cells or in comparison to haploid cells under N-depletion or upon entering stationary phase in replete cultures (Supplemental Figure J). In conclusion, diploid cells appear to resist N-depletion better, while haploid cells appear to resist P-depletion better. The haploid stage possesses only half the amount of DNA, and its tolerance against P-depletion may thus be due to the lower P-demand for DNA replication as well as RNA synthesis (Lewis, 1985; Loladze and Elser, 2011) and may be directly connected to the distinct niche-occupations of the two life-cycle stages (Von Dassow et al., 2009; Rokitta et al., 2011).

Structure of the Transcriptomic Response

Microarray data revealed that distinct, but functionally consistent sets of genes responded in haploid and diploid cells (**Figure 2**; Supplemental Table 1). We report data for both time points, but for simplicity, we argue along the data of the 'Full depletion' response, where the observed transcriptomic responses are most clearly represented.

In response to external P-depletion, 3904 genes (68.5% of all the significantly regulated genes in this stage) changed expression only in the diploid stage (**Figure 2**). 2187 genes (55% of all significantly regulated genes in this stage) were differentially expressed only in the haploid stage. 1586 genes (20% of all significantly regulated genes) experienced unidirectional expression changes in both life-cycle stages. A residual of 212 genes (2.7% of all significantly regulated genes) showed an incoherent or contradictory response between the life-cycle stages. These patterns of expression are consistent with the transcriptomic patterns observed in response to N-depletion (Rokitta et al., 2014) and derive from the tripartite genome that accompanies life-cycling: One portion of the genome seems to be a basic 'operating system' , required by both stages, whereas other large portions follow highly stage-specific expression patterns and appear to shape the two life-cycle stages structurally, functionally as well as ecologically (Von Dassow et al., 2009; Rokitta et al., 2011).

The expression patterns at the two assessed time points 'Early depletion' and 'Full depletion' (**Figure 2**) are functionally coherent, the expression patterns share 68 to 75 percent of the regulated features in diploid and haploid stages, respectively. This is very similar to the pattern observed under N-depletion (Rokitta et al., 2014): Under both, P- and N-depleted conditions, the functional coherence between the investigated time points suggests that the metabolism undergoes a comprehensive and more or less immediate re-constellation, rather than executing a sequential series of distinguishable countermeasures. Furthermore, the transcriptomic responses, both to P-depletion (this study) and to N-depletion (Rokitta et al., 2014), are strongly amplified over time, as is apparent from increasing fold-change values, indicating that the transcriptomic responses are coupled in their intensity to the progressive character of cell starvation.

In the experiment, the cellular growth arrest occurred within 36 h after extracellular P was depleted below detectable levels (**Figures 1A–C**), very similar to the time scale of growth arrest after N-depletion (Rokitta et al., 2014). To explore the degree to which the responses to N- and P-depletion share a genetic basis, we compared the transcriptomic responses under full P-depletion to those reported earlier under full N-depletion (Rokitta et al., 2014). Indeed, the responses to N- and P-depletion within each life-cycle stage showed a significant overlap, with 63 to 68 percent of the regulated genes being essentially the same (**Figure 3**). In fact, these specific transcriptomic responses of the particular stages toward N- and P-depletion are much more similar and coherent than the responses of the two life-cycle stages toward one particular depletion scenario (**Figure 2**, see also **Figure 3** in Rokitta et al., 2014). In other words, there is less difference between the two depletion responses *within* one life-cycle stage than there is difference *between* the two stages in response to a single nutrient-depletion condition.

General Responses to P- and N-depletion

The observed response to P-depletion was compared in more detail to the response to N-depletion that was reported earlier, specifically by looking at the 162 exemplarily selected genes that were interpreted to constitute the cellular response to N-depletion in *E. huxleyi* (Rokitta et al., 2014) and by including 33 further genes (Supplemental Table 2). In fact, 161 out of the 162 previously highlighted genes were regulated in the same direction in response to P-depletion as well as N-depletion, suggesting that the major re-constellations of metabolism are highly similar in both scenarios. These re-constellations include the prominent down-regulation of genes related to RNA

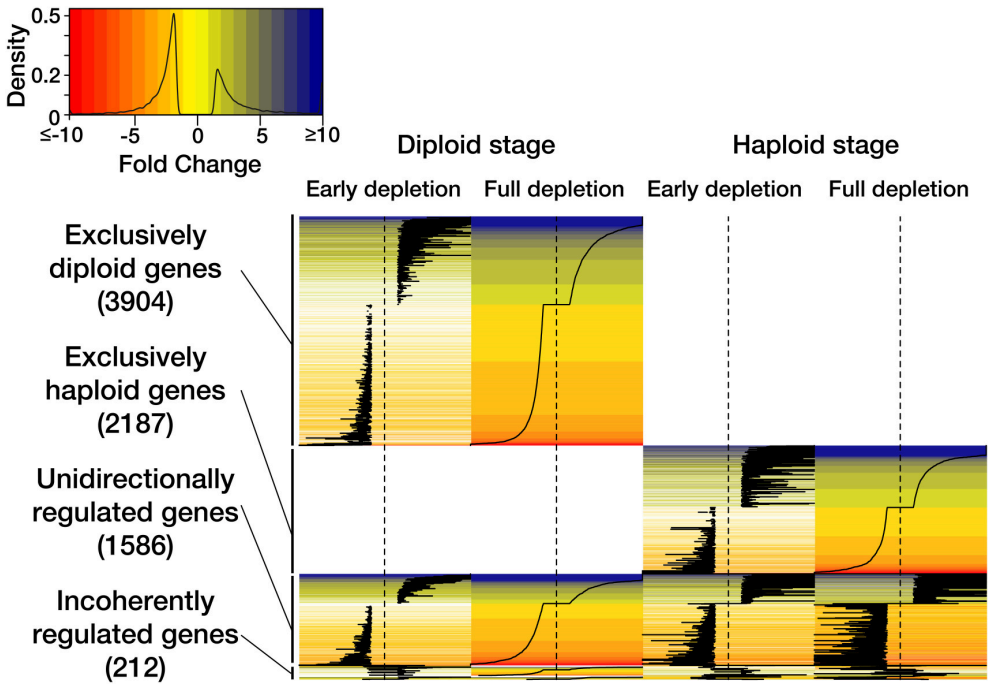

FIGURE 2 | Heat map representation of the observed transcriptomic responses to P-depletion in haploid and diploid *Emiliania huxleyi*. The legend contains color-coding of 'fold-change' expression values, the density function reflects data distribution. The heat map depicts the time course of P-depletion in haploid and diploid individuals and the generic as well as stage-specific usage of genes.

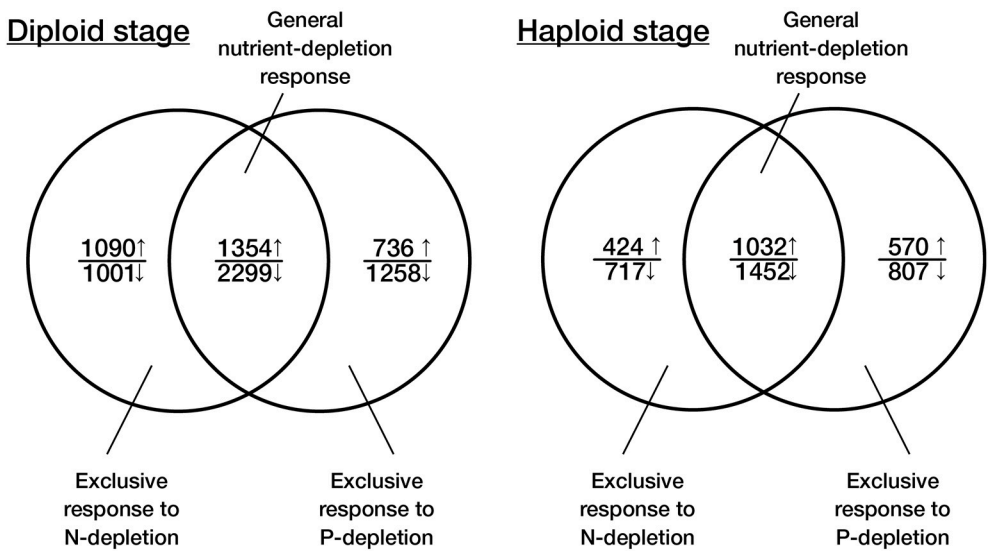

FIGURE 3 | Venn diagram representation of the functional overlap between the transcriptomic responses to N- and P-depletion in the two life-cycle stages of *Emiliania huxleyi*. The data on the responses toward N-depletion is taken from Rokitta et al. (2014).

and protein biosynthesis, photosynthetic light reactions, and mitochondrial ATP generation as well as the restructuring of carbon fluxes and the induction of MQO-supported reduction of the quinone pool (Rokitta et al., 2014). As under N-depletion, we observed significant regulations in the biochemical pathways of lipid buildup and breakdown, supposedly reflecting an enhanced lipid turnover. Especially notable was that both, P- and N-depletion induced largely the same re-constellations of genes related to N metabolism, i.e., decreased expression of genes of the ornithine-urea-cycle (OUC) and massive induction of proline oxidase (POX). This is likely due to the tight stoichiometric coupling of N and P metabolism, and thus

may explain the near-absence of NO_3^- consumption under P-depletion (**Figure 1D**). However, the prominent upregulation of POX also under P-depletion implies that this enzyme not only functions in N budgeting (as interpreted in Rokitta et al., 2014), but has a superior regulatory role in arresting the cell-cycle, as is also suggested by numerous recent results from cancer research with animal cells (Liu et al., 2009; Pandhare et al., 2009; Phang et al., 2012). Beyond its role in the generation of reactive oxygen species (Pandhare et al., 2009; Phang et al., 2012), POX possibly also contributes to the maintenance of the mitochondrial inner membrane polarization to counteract premature cell death as a consequence of a mitochondrial permeability transition (Gottlieb et al., 2003; Bernardi, 2013; Malhotra et al., 2013).

Another interesting finding in the context of nutrient-depletion is the significant activation of the methylglyoxal (MG) pathway, the so-called 'glycolytic bypass.' This ubiquitous pathway circumvents the conventional oxidative part of glycolysis and facilitates the conversion of dihydroxyacetonephosphate into pyruvate via lactate, with e.g., glutathione as reductant carrier and without the generation of ATP (Chakraborty et al., 2014). This pathway is increasingly used also in animal cells, in situations where glycolytic intermediates accumulate in the cell, e.g., due to excess sugar input and/or decreased glycolytic flux. Also, when NAD and inorganic phosphate (required for conventional glycolysis) are low due to depletion in N or P, the glycolytic bypass can to a certain extent continue the oxidation of dihydroxyacetonephosphate. However, instead of just being an alternative route, increasing cellular levels of MG also promote the cell-cycle arrest and various forms of cell death (Kalapos, 1999): MG is a potent glycating agent that irreversibly modifies and inactivates proteins, and is therefore also used as an effective cytostatic in chemotherapy (Chakraborty et al., 2014). The diploid stage downregulates cytosolic and plastidic forms of glyoxalase I (GJ07554, GJ11585, GJ09709), but both life-cycle stages additionally induce other cytosolic and mitochondrial glyoxalase II enzymes (GJ08445, GJ02232, GJ02627), regulations that likely increase cellular levels of MG and contribute to the cell-cycle arrest. To convert the resulting D-lactate to pyruvate, cells of both life-cycle stages upregulate corresponding D-lactate dehydrogenases (GJ20429, GJ12287, GJ17732, GJ11998). Interestingly, the upregulation of these dehydrogenases occurs only under P-limitation. It is known that the MG pathway is induced in other microalgae when inorganic phosphate concentrations are low (Frischkorn et al., 2014), and that an enhanced operation of this pathway can liberate inorganic phosphate from glycolytic intermediates and produce pyruvate, even when levels of NAD and inorganic P are low (Chakraborty et al., 2014). The induction of the lactate dehydrogenases is thus likely an additional measure to relieve the limitation in inorganic phosphate in the cytosol in situations of external nutrient depletion.

The dataset also indicates the induction of autophagic genes (e.g., regulation of autophagy-related enzymes ATG 1, 8, 9. and 10; GJ17478, GJ05745, GJ00141, GJ03622), as well as proapoptotic (e.g., diverse metacaspases involved in the regulation of apoptosis; GJ25353, GJ01565, GJ03128) and also antiapoptotic genes (e.g., apoptosis-inhibitor protein; GJ03892). These expression patterns reflect cellular changes that liberate organically bound nutrients by the degradation of cellular structures for resource re-allocation and at the same time reduce the overall metabolic demands, by decreasing the number of organelles. As suggested before (Shemi et al., 2016), the nutrient depletion promotes metabolic re-constellations and, as a consequence, also versatile auto-destructive cell remodeling processes that need to be kept in check by the cell to avoid, or at least delay, the otherwise inevitable self-destruction (Eguchi et al., 1997; Tsujimoto and Shimizu, 2005; Jiménez et al., 2009; Chakraborty et al., 2014; Bidle, 2015).

Exclusive Responses to P- and N-depletion

In contrast to the described 'general depletion responses', in which the cells stop growing and enter senescence, sets of genes were exclusively upregulated only in response to either P- or N-depletion (**Figure 3**), which appear to modulate the generic metabolic readjustments according to the required nutrient.

In the exclusive response to P-depletion, both stages prominently induced machinery serving the scavenging and storage of the depleted nutrient: Phosphate depletion induced the expression of inorganic phosphate transporters in both diploid and haploid cells, as was earlier observed in diploid *E. huxleyi* (Dyhrman et al., 2006). While some of these transporters were upregulated in both stages (GJ07903 and GJ17289), others were induced only in the diploid phase (GJ07431, GJ19080) or the haploid phase (GJ00052, GJ18265). The diploid stage induced a protein involved in vacuolar deposition of polyphosphates (GJ00534) and strongly induced an alkaline phosphatase (GJ22399, GJ14355) that supports efficient cleavage of inorganic P from dissolved external organic sources. This enzyme of *E. huxleyi* has been observed to possess an extraordinarily high affinity and is typically discussed as one of the prime measures of this species to maintain its P budget in environments where inorganic P is scarce (Riegman et al., 2000; Dyhrman et al., 2006). The haploid life-cycle stage, however, expressed only an *acidic* phosphatase (GJ11194), a type of enzyme that is typically present in digestive organelles with low pH, like lysosomes (Braun et al., 1989). Apparently, both stages take measures to increase P uptake, but the induced sets partly differ between the stages. It might thus be interpreted that, in response to low inorganic P, the diploid stage increases the uptake of PO_4^{3-} cleaved off external organic P, whereas the haplont also increases the utilization of PO_4^{3-} that derives from the lysosomal digestion of internalized (or autophagically derived) organic matter. Indeed, it was already hypothesized that phagotrophic feeding of the haploid stage could constitute an adaptation to their natural habitat, i.e., post-bloom situations with low concentrations of inorganic nutrients, but comparably high concentrations of particulate organic matter (Rokitta et al., 2011). Capacities for the uptake of dissolved organics are inherent to all cells and might facilitate also an auxiliary *osmotrophic*, ultimately even *dasmotrophic* way of nutrition (Estep and MacIntyre, 1989), supporting cell survival when inorganic nutrients are depleted.

In the exclusive response to N-depletion, diploid cells in particular downregulated multiple subunits of respiratory complex I (GJ11336, GJ16883, GJ14395, GJ15869, GJ05219,

GJ00231), indicating that the rerouting of electrons to circumvent complex I is a necessity under N-depletion only (Rokitta et al., 2014). This may derive from the fact that the complex' substrates (NADH) and redox cofactors (FAD) can be considerably decreased under N-depletion; under such conditions, electrons might be rather transferred directly into the electron transfer chain, e.g., via POX or MQO, as seen in the global depletion response, thereby decreasing the requirements for soluble reductant carriers. Thus, the downregulation of complex I appears as an additional measure to decrease metabolic N demands and to strengthen and support the effects of the other cellular readjustments.

These data show that in addition to the general arrest of cell-cycling and the transition to senescence, *E. huxleyi* exhibits well-tuned specific responses to the environmental nutrient status that not only streamline metabolism and cellular architecture for low nutrient demands but also maximize the scavenging of the nutrient that is particularly limiting. The stage-specific usage of distinct sets of genes that facilitate the same or similar metabolic functions suggests that both life-cycle stages attempt to maintain metabolic balance in response to nutrient depletion, but with different machinery. Also numerically, the diplont regulates a much higher number of genes than the haploid stage, confirming differences in regulation patterns between stages (Rokitta et al., 2011). Unfortunately, for most genes that show stage-specific regulation patterns, there is no homology information available, which disables the interpretation of these stage-specific responses. Lastly, here we have only analyzed genes that were present in the reference genome of strain CCMP1516 (Read et al., 2013). This improved our ability to perform functional annotation and to focus on genes common to many *E. huxleyi* genotypes and ecotypes. However, it has been shown that stage-specific genes can be differentially present in different *E. huxleyi* genomes, with strain CCMP1516 having lost 10% of 1N-specific genes present in the strain used in this study, and 59% of these had no detectable homology to known genes (Von Dassow et al., 2015). Our observations support the idea that these genes without known homologies may play important roles in niche occupation and life-cycle constraints (Von Dassow et al., 2009, 2015; Rokitta et al., 2011; Read et al., 2013). Many of the genes showing exclusive expression in one life-cycle stage or the other may, for example, code for non-translated, regulatory RNAs or small structural protein factors that are not well described yet, or for proteins that are unique to haptophytes or coccolithophores.

Synthesis

From this and a number of other recent datasets, it becomes clear that when cells face nutrient depletion, ancient and highly conserved responses are commonly triggered to downregulate RNA and protein synthesis (Wagner et al., 2013), arrest cell-cycling, reconfigure metabolic pathways (**Figure 4**), and induce efficient recycling and scavenging to optimize nutrient usage and acquisition (Hillebrand et al., 2013). These interpretations are corroborated, e.g., by a recent proteome study on *E. huxleyi*, in which N- and P-depletion induced the same canonical responses to re-structure metabolism, but differential specific responses to increase the cellular budgets of the missing nutrient (McKew et al., 2015). These responses to N- and P-depletion described in *E. huxleyi* can also be seen in other phytoplankton, e.g., the related prymnesiophyte *Prymnesium parvum* triggers more or less the same response (Liu et al., 2015), including the arrest of cell-cycling, differential regulation of the OUC, increased internal turnover of proteins and lipids as well as effective scavenging of nutrients. Also more distantly related phytoplankton genera seem to apply these mechanisms: Comparable responses to nutrient-depletion have been observed in the dinoflagellate *Karenia brevis*, although its P-depletion response was much less pronounced than observed here (Morey et al., 2011). In the N-starved diatom *Phaeodactylum tricornutum*, genes related to the OUC were regulated in the same manner as observed in N- and P-starved *E. huxleyi* cells (Allen et al., 2011, this study; Rokitta et al., 2014). It has also been shown that this diatom experiences highly similar modifications of its lipidome in response to both depletion scenarios (Abida et al., 2015), indicating that, in diatoms as well, P- and N-depletion trigger more or less the same biochemical program. Likewise, in the pelagophyte *Aureococcus*, the arrest of cell-cycling, extensive nutrient scavenging, internal metabolic re-constellations, as well as a prominent induction the MG pathway were observed (Frischkorn et al., 2014), underlining the common conserved cell-biological basis of unicellular eukaryotes.

The high similarity of all these expression patterns across different phytoplankton taxa as well as the tight conservation of parts of the involved machinery from protists to humans (Liu et al., 2009; Phang et al., 2012; Chakraborty et al., 2014) shows that the molecular mechanisms that balance cell proliferation vs. cell-cycle arrest and senescence are still operative, even across distant lineages and evolutionary histories.

In nature, there are many ecological processes and adaptive mechanisms occurring simultaneously when a phytoplankton bloom enters senescence, e.g., recycling of nutrients by grazers (Eppley and Peterson, 1979), viral termination (Frada et al., 2008), or mutual facilitation (John et al., 2015). However, the reductionist, artificial laboratory system used here elucidated a genetic senescence-transition program that appears to constitute another, possibly quite underestimated mechanism. Its wide genetic occurrence and conservation among distant groups of marine protists suggests that it is and has been also an adaptive strategy for phytoplankton: Cells, confronted with life-threatening nutrient depletion struggle for survival by inducing the described 'emergency-program' to delay their own death as long as possible. Cells that fail first in doing so will die and set free organic nutrients that are readily taken up by more persistent competitors, including their conspecifics. Over longer timescales, this mechanism will promote selection for very enduring cells and thus may be an important factor shaping the genetics of phytoplankton populations. Also, it delivers an additional explanation for the often observed phenomena of increased cell division rates despite a constantly high portion of dead and dying cells when phytoplankton occupy nutrient-poor environments (Agustí et al., 1998; Agustí and Sánchez, 2002; Bidle, 2015).

Besides the strong parallels between the life-cycle stages with respect to their overall behavior under nutrient limitation,

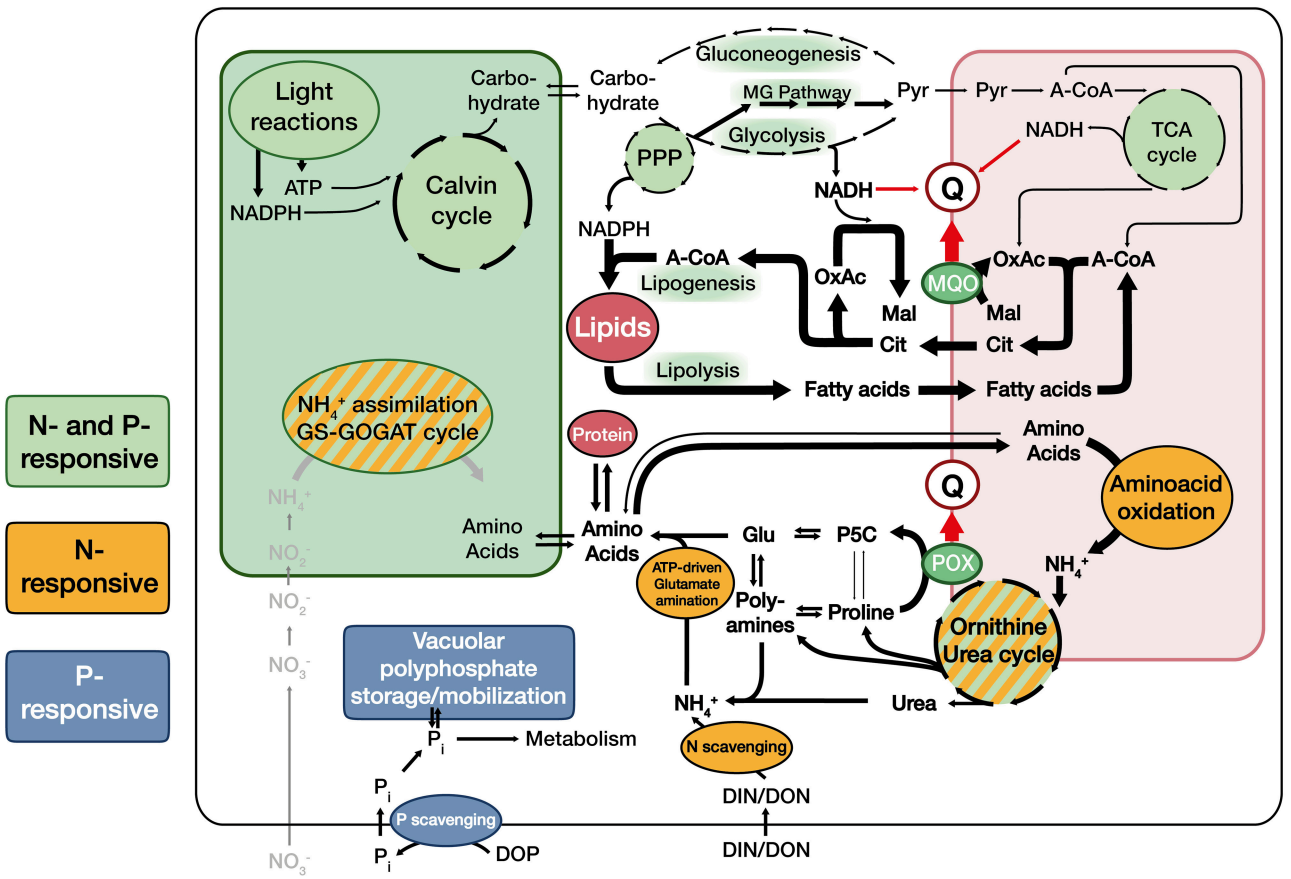

FIGURE 4 | Proposed generalized metabolic constellations in *Emiliania huxleyi* under nutrient-depletion: Under nutrient-depletion, photosynthetic light reactions, and carbon fixation are minimized. As a consequence, carbon input into the cell and thus the flux through glycolysis and the TCA cycle are reduced. Cells strongly induce the citrate-shuttle that exports acetyl-CoA into the cytoplasm and increase the relative intensity of lipid turnover (synthesis as well as oxidation), which provides required sinks for reduction equivalents. To facilitate electron input into the quinone-pool (Q) under these adverse flux conditions, cells make use of a malate:quinone oxidoreductase (MQO). Mitochondrial amino acid oxidation is increased, while enzymes of the ornithine-urea-cycle (OUC) and connected reactions are throttled, putatively leading to a accumulation of OUC intermediates, polyamines and proline relative to common aminoacids. The oxidation of proline to pyrroline-5-carboxylate (P5C) by proline oxidase (POX) appears to be a major entryway for reductants into Q when nutrients are scarce and protein machinery is eroded. Especially the diploid stage induces machinery to scavenge external (in)organic N and P (orange and blue shade).

they exhibited key transcriptomic and physiological differences (e.g., photosynthetic efficiency measures suggested that diploid cells are more resistant to N-depletion whereas haploid cells are more resistant to P-depletion). Importantly, there is a numerically significant portion of genes that are differentially regulated between the stages, for which no gene homology information is available. These under-investigated genes may play important roles in defining the ploidy stages as such, and their distinct ecological niches, and attention should be paid in the future to elucidate the functions of these transcripts.

CONCLUSION

The canonical responses of diverse protistan taxa to P- and N-depletion give rise to an emerging picture about how phytoplankton transitions into senescence to ensure population survival in oligotrophic environments. Critical hallmarks of the transition are the arrest of cell-cycling, re-constellation of central carbon metabolism as well as effective scavenging of nutrients, supported by intense cellular turnover. Ensuring survival, it is a crucial mechanism on which evolution continuously acts and thereby streamlines phytoplankton species for optimal persistence in their habitats. While this strategy is true for many, if not all phytoplankton, it appears that *E. huxleyi*'s outstanding endurance is owed especially to its versatile and uniquely high-affinity uptake systems as well as the efficient NAD-independent malate-oxidation that seems to be lacking from most other protistan taxa.

AUTHOR CONTRIBUTIONS

SR contributed to planning the study, carried out the experiments, processed data, and drafted the manuscript;

PD and UJ devised the study design, helped to carry out experiments and contributed to writing the manuscript; BR helped to carry out experiments and contributed to writing the manuscript.

FUNDING

SR was funded by the German Ministry for Education and Research under grant no. 031A518C. PD received a supported by a Marie Curie International Incoming Fellowship within the 7th European Community Framework Programme (Grant PIIF-GA-2008-221812). BR and SR further received funding from the European Research Council under the European Community's Seventh Framework Programme (FP7/2007–2013)/ERC grant agreement no. [205150]. We like to thank Hiroyuki Ogata who generously contributed sequence information for array construction and Daniela Ewe for her help in sample taking and processing.

SUPPLEMENTARY MATERIAL

The Supplementary Material for this article can be found online at: http://journal.frontiersin.org/article/10.3389/fmars.2016.00109

REFERENCES

Abida, H., Dolch, L.-J., Meï, C., Villanova, V., Conte, M., Block, M.A., et al. (2015). Membrane glycerolipid remodeling triggered by nitrogen and phosphorus starvation in phaeodactylum tricornutum. *Plant Physiol.* 167, 118–136. doi: 10.1104/pp.114.252395

Agustí, S., and Sánchez, M. C. (2002). Cell viability in natural phytoplankton communities quantified by a membrane permeability probe. *Limnol. Oceanogr.* 47, 818–828. doi: 10.4319/lo.2002.47.3.0818

Agustí, S., Satta, M. P., Mura, M. P., and Benavent, E. (1998). Dissolved esterase activity as a tracer of phytoplankton lysis: evidence of high phytoplankton lysis rates in the northwestern Mediterranean. *Limnol. Oceanogr.* 43, 1836–1849.

Allen, A. E., Dupont, C. L., Obornik, M., Horak, A., Nunes-Nesi, A., Mccrow, J. P., et al. (2011). Evolution and metabolic significance of the urea cycle in photosynthetic diatoms. *Nature* 473, 203–207. doi: 10.1038/nature10074

Bakun, A., Field, D. B., Redondo-Rodriguez, A. N. A., and Weeks, S. J. (2010). Greenhouse gas, upwelling-favorable winds, and the future of coastal ocean upwelling ecosystems. *Glob. Chang. Biol.* 16, 1213–1228. doi: 10.1111/j.1365-2486.2009.02094.x

Benjamini, Y., and Hochberg, Y. (1995). Controlling the false discovery rate - a practical and powerful approach to multiple testing. *J. R. Stat. Soc. Ser. B Methodol.* 57, 289–300.

Bernardi, P. (2013). The mitochondrial permeability transition pore: a mystery solved? *Front. Physiol.* 4:95. doi: 10.3389/fphys.2013.00095

Bidle, K. D. (2015). The molecular ecophysiology of programmed cell death in marine phytoplankton. *Ann. Rev. Mar. Sci.* 7, 341–375. doi: 10.1146/annurev-marine-010213-135014

Braun, M., Waheed, A., and Von Figura, K. (1989). Lysosomal acid phosphatase is transported to lysosomes via the cell surface. *EMBO J.* 8, 3633–3640.

Chakraborty, S., Karmakar, K., and Chakravortty, D. (2014). Cells producing their own nemesis: understanding methylglyoxal metabolism. *IUBMB Life* 66, 667–678. doi: 10.1002/iub.1324

Conesa, A., Götz, S., García-Gómez, J. M., Terol, J., Talón, M., and Robles, M. (2005). Blast2GO: a universal tool for annotation, visualization and analysis in functional genomics research. *Bioinformatics* 21, 3674–3676. doi: 10.1093/bioinformatics/bti610

Dickson, A. G. (1981). An exact definition of total alkalinity and a procedure for the estimation of alkalinity and total inorganic carbon from titration data. *Deep Sea Res. Part I Oceanogr. Res. Pap.* 28, 609–623. doi: 10.1016/0198-0149(81)90121-7

Doney, S. C., Ruckelshaus, M., Duffy, J. E., Barry, J. P., Chan, F., English, C. A., et al. (2012). Climate change impacts on marine ecosystems. *Ann. Rev. Mar. Sci.* 4, 11–37. doi: 10.1146/annurev-marine-041911-111611

Dyhrman, S. T., Haley, S. T., Birkeland, S. R., Wurch, L. L., Cipriano, M. J., and Mcarthur, A. G. (2006). Long serial analysis of gene expression for gene discovery and transcriptome profiling in the widespread marine coccolithophore *Emiliania huxleyi*. *Appl. Environ. Microbiol.* 72, 252–260. doi: 10.1128/AEM.72.1.252-260.2006

Eguchi, Y., Shimizu, S., and Tsujimoto, Y. (1997). Intracellular ATP levels determine cell death fate by apoptosis or necrosis. *Cancer Res.* 57, 1835–1840.

Eppley, R. W., and Peterson, B. J. (1979). Particulate organic matter flux and planktonic new production in the deep ocean. *Nature* 282, 677–680. doi: 10.1038/282677a0

Estep, K. W., and MacIntyre, F. (1989). Taxonomy, life cycle, distribution and dasmotrophy of *Chrysochromulina*: a theory accounting for scales, haptonema, muciferous bodies and toxicity. *Mar. Ecol. Progress Ser.* 57, 11–21. doi: 10.3354/meps057011

Field, C. B., Behrenfeld, M. J., Randerson, J. T., and Falkowski, P. (1998). Primary production of the biosphere: integrating terrestrial and oceanic components. *Science* 281, 237–240. doi: 10.1126/science.281.5374.237

Flynn, K. J. (2008). The importance of the form of the quota curve and control of non-limiting nutrient transport in phytoplankton models. *J. Plankton Res.* 30, 423–438. doi: 10.1093/plankt/fbn007

Frada, M., Probert, I., Allen, M. J., Wilson, W. H., and De Vargas, C. (2008). The "Cheshire Cat" escape strategy of the coccolithophore *Emiliania huxleyi* in response to viral infection. *PNAS* 105, 15944–15949. doi: 10.1073/pnas.0807707105

Frischkorn, K. R., Harke, M. J., Gobler, C. J., and Dyhrman, S. T. (2014). De novo assembly of *Aureococcus anophagefferens* transcriptomes reveals diverse responses to the low nutrient and low light conditions present during blooms. *Front. Microbiol.* 5:375. doi: 10.3389/fmicb.2014.00375

Gottlieb, E., Armour, S. M., Harris, M. H., and Thompson, C. B. (2003). Mitochondrial membrane potential regulates matrix configuration and cytochrome c release during apoptosis. *Cell Death Differ.* 10, 709–717. doi: 10.1038/sj.cdd.4401231

Green, J. C., Course, P. A., and Tarran, G. A. (1996). The life-cycle of *Emiliania huxleyi*: a brief review and a study of relative ploidy levels analysed by flow cytometry. *J. Mar. Syst.* 9, 33–44. doi: 10.1016/0924-7963(96)00014-0

Guillard, R. R. L., and Ryther, J. H. (1962). Studies of marine planktonic diatoms. *Can. J. Microbiol.* 8, 229–239. doi: 10.1139/m62-029

Hillebrand, H., Steinert, G., Boersma, M., Malzahn, A., Meunier, C. L., Plum, C., et al. (2013). Goldman revisited: faster-growing phytoplankton has lower N:P and lower stoichiometric flexibility. *Limnol. Oceanogr.* 58, 2076–2088. doi: 10.4319/lo.2013.58.6.2076

Jiménez, C., Capasso, J. M., Edelstein, C. L., Rivard, C. J., Lucia, S., Breusegem, S., et al. (2009). Different ways to die: cell death modes of the unicellular chlorophyte Dunaliella viridis exposed to various environmental stresses are mediated by the caspase-like activity DEVDase. *J. Exp. Bot.* 60, 815–828. doi: 10.1093/jxb/ern330

John, U., Tillmann, U., Hülskötter, J., Alpermann, T. J., Wohlrab, S., and Van de Waal, D. B. (2015). Intraspecific facilitation by allelochemical mediated grazing protection within a toxigenic dinoflagellate population. *Proc. R. Soc. Lond. B Biol. Sci.* 282:20141268. doi: 10.1098/rspb.2014.1268

Kalapos, M. P. (1999). Methylglyoxal in living organisms: chemistry, biochemistry, toxicology and biological implications. *Toxicol. Lett.* 110, 145–175. doi: 10.1016/S0378-4274(99)00160-5

Kather, B., Stingl, K., Van Der Rest, M. E., Altendorf, K., and Molenaar, D. (2000). Another unusual type of citric acid cycle enzyme in *Helicobacter*

pylori: the malate:quinone oxidoreductase. *J. Bacteriol.* 182, 3204–3209. doi: 10.1128/JB.182.11.3204-3209.2000

Keeling, P. J., Burki, F., Wilcox, H. M., Allam, B., Allen, E. E., Amaral-Zettler, L. A., et al. (2014). The Marine Microbial Eukaryote Transcriptome Sequencing Project (MMETSP): illuminating the functional diversity of eukaryotic life in the oceans through transcriptome sequencing. *PLoS Biol.* 12:e1001889. doi: 10.1371/journal.pbio.1001889

Kegel, J. U., John, U., Valentin, K., and Frickenhaus, S. (2013). Genome variations associated with viral susceptibility and calcification in *Emiliania huxleyi*. *PLoS ONE* 8:e80684. doi: 10.1371/journal.pone.0080684

Klaas, C., and Archer, D. E. (2002). Association of sinking organic matter with various types of mineral ballast in the deep sea: implications for the rain ratio. *Global Biogeochem. Cycles* 16, 1116–1130. doi: 10.1029/2001GB001765

Lessard, E. J., Merico, A., and Tyrrell, T. (2005). Nitrate: phosphate ratios and *Emiliania huxleyi* blooms. *Limnol. Oceanogr.* 50, 1020–1024. doi: 10.4319/lo.2005.50.3.1020

Lewis, W. M. Jr. (1985). Nutrient scarcity as an evolutionary cause of haploidy. *Am. Nat.* 125, 692–701. doi: 10.1086/284372

Liu, Y., Borchert, G. L., Donald, S. P., Diwan, B. A., Anver, M., and Phang, J. M. (2009). Proline oxidase functions as a mitochondrial tumor suppressor in human cancers. *Cancer Res.* 69, 6414–6422. doi: 10.1158/0008-5472.CAN-09-1223

Liu, Z., Koid, A. E., Terrado, R., Campbell, V., Caron, D. A., and Heidelberg, K. B. (2015). Changes in gene expression of *Prymnesium parvum* induced by nitrogen and phosphorus limitation. *Front. Microbiol.* 6:631. doi: 10.3389/fmicb.2015.00631

Löbl, M., Cockshutt, A. M., Campbell, D., and Finkel, Z. V. (2010). Physiological basis for high resistance to photoinhibition under nitrogen depletion in E*miliania huxleyi*. *Limnol. Oceanogr.* 55, 2150–2160. doi: 10.4319/lo.2010.55.5.2150

Loladze, I., and Elser, J. J. (2011). The origins of the Redfield nitrogen-to-phosphorus ratio are in a homoeostatic protein-to-rRNA ratio. *Ecol. Lett.* 14, 244–250. doi: 10.1111/j.1461-0248.2010.01577.x

Malhotra, K., Sathappa, M., Landin, J. S., Johnson, A. E., and Alder, N. N. (2013). Structural changes in the mitochondrial Tim23 channel are coupled to the proton-motive force. *Nat. Struct. Mol. Biol.* 20, 965–972. doi: 10.1038/nsmb.2613

Mckew, B. A., Davey, P., Finch, S. J., Hopkins, J., Lefebvre, S. C., Metodiev, M. V., et al. (2013). The trade-off between the light-harvesting and photoprotective functions of fucoxanthin-chlorophyll proteins dominates light acclimation in *Emiliania huxleyi* (clone CCMP 1516). *New Phytol.* 200, 74–85. doi: 10.1111/nph.12373

McKew, B. A., Metodieva, G., Raines, C. A., Metodiev, M. V., and Geider, R. J. (2015). Acclimation of *Emiliania huxleyi* (1516) to nutrient limitation involves precise modification of the proteome to scavenge alternative sources of N and P. *Environ. Microbiol.* 17, 4050–4062. doi: 10.1111/1462-2920.12957

Mohan, R., Mergulhao, L. P., Guptha, M. V. S., Rajakumar, A., Thamban, M., Anilkumar, N., et al. (2008). Ecology of coccolithophores in the Indian sector of the Southern Ocean. *Mar. Micropaleontol.* 67, 30–45. doi: 10.1016/j.marmicro.2007.08.005

Molenaar, D., Van Der Rest, M. E., and Petrović, S. (1998). Biochemical and genetic characterization of the membrane-associated malate dehydrogenase (acceptor) from *Corynebacterium glutamicum*. *Eur. J. Biochem.* 254, 395–403. doi: 10.1046/j.1432-1327.1998.2540395.x

Morey, J. S., Monroe, E. A., Kinney, A. L., Beal, M., Johnson, J. G., Hitchcock, G. L., et al. (2011). Transcriptomic response of the red tide dinoflagellate, *Karenia brevis*, to nitrogen and phosphorus depletion and addition. *BMC Genomics* 12:346. doi: 10.1186/1471-2164-12-346

Paasche, E. (1998). Roles of nitrogen and phosphorus in coccolith formation in *Emiliania huxleyi* (Prymnesiophyceae). *Eur. J. Phycol.* 33, 33–42. doi: 10.1080/09670269810001736513

Paasche, E. (2002). A review of the coccolithophorid *Emiliania huxleyi* (Prymnesiophyceae), with particular reference to growth, coccolith formation, and calcification-photosynthesis interactions. *Phycologia* 40, 503–529. doi: 10.2216/i0031-8884-40-6-503.1

Pandhare, J., Donald, S. P., Cooper, S. K., and Phang, J. M. (2009). Regulation and function of proline oxidase under nutrient stress. *J. Cell. Biochem.* 107, 759–768. doi: 10.1002/jcb.22174

Phang, J. M., Liu, W., Hancock, C., and Christian, K. J. (2012). The proline regulatory axis and cancer. *Front. Oncol.* 2:60. doi: 10.3389/fonc.2012.00060

Pierrot, D. E., Lewis, E., and Wallace, D. W. R. (2006). "MS Excel program developed for CO2 system calculations," in *Carbon Dioxide Information Analysis Center* (Oak Ridge, TN: *Oak Ridge National Laboratory (ORNL)*).

Read, B. A., Kegel, J., Klute, M. J., Kuo, A., Lefebvre, S. C., Maumus, F., et al. (2013). Pan genome of the phytoplankton *Emiliania* underpins its global distribution. *Nature* 499, 209–213. doi: 10.1038/nature12221

Riegman, R., Stolte, W., Noordeloos, A. A.M., and Slezak, D. (2000). Nutrient uptake and alkaline phosphatase (EC 3.1.3.1) activity of *Emiliania huxley*$_i$ (Prymnesiophyceae) during growth under N and P limitation in continuous cultures. *J. Phycol.* 36, 87–96. doi: 10.1046/j.1529-8817.2000.99023.x

Rokitta, S. D., De Nooijer, L. J., Trimborn, S., De Vargas, C., Rost, B., and John, U. (2011). Transcriptome analyses reveal differential gene expression patterns between life-cycle stages of *Emiliania huxleyi* (Haptophyta) and reflect specialization to different ecological niches. *J. Phycol.* 47, 829–838. doi: 10.1111/j.1529-8817.2011.01014.x

Rokitta, S. D., John, U., and Rost, B. (2012). Ocean Acidification affects redox-balance and ion-homeostasis in the life-cycle stages of *Emiliania huxleyi*. *PLoS ONE* 7:e52212. doi: 10.1371/journal.pone.0052212

Rokitta, S. D., and Rost, B. (2012). Effects of CO_2 and their modulation by light in the life-cycle stages of the coccolithophore *Emiliania huxleyi*. *Limnol. Oceanogr.* 57, 607–618. doi: 10.4319/lo.2012.57.2.0607

Rokitta, S. D., Von Dassow, P., Rost, B., and John, U. (2014). *Emiliania huxleyi* endures N-limitation with an efficient metabolic budgeting and effective ATP synthesis. *BMC Genomics* 15:1051. doi: 10.1186/1471-2164-15-1051

Rost, B., and Riebesell, U. (2004). "Coccolithophores and the biological pump: responses to environmental changes," in *Coccolithophores - From Molecular Processes to Global Impact*, eds H. R. Thierstein and J. R. Young (Heidelberg: Springer), 99–125.

Shemi, A., Schatz, D., Fredricks, H. F., Van Mooy, B. A. S., Porat, Z., and Vardi, A. (2016). Phosphorus starvation induces membrane remodeling and recycling in *Emiliania huxleyi*. *New Phytol.* doi: 10.1111/nph.13940. [Epub ahead of print].

Steinacher, M., Joos, F., Frölicher, T. L., Bopp, L., Cadule, P., Cocco, V., et al. (2010). Projected 21st century decrease in marine productivity: a multi-model analysis. *Biogeosciences* 7, 979–1005. doi: 10.5194/bg-7-979-2010

Stoll, H. M., Ruiz Encinar, J., Ignacio Garcia Alonso, J., Rosenthal, Y., Probert, I., and Klaas, C. (2001). A first look at paleotemperature prospects from Mg in coccolith carbonate: cleaning techniques and culture measurements. *Geochem. Geophys. Geosyst.* 2, 1047. doi: 10.1029/2000GC000144

Stoll, M. H. C., Bakker, K., Nobbe, G. H., and Haese, R. R. (2001). Continuous-flow analysis of dissolved inorganic carbon content in seawater. *Anal. Chem.* 73, 4111–4116. doi: 10.1021/ac010303r

Strickland, J. D. H., and Parsons, T. R. (1972). *Practical Handbook of Seawater Analysis*. Ottawa, ON: Fisheries Research Board of Canada.

Tsujimoto, Y., and Shimizu, S. (2005). Another way to die: autophagic programmed cell death. *Cell Death Differ.* 12, 1528–1534. doi: 10.1038/sj.cdd.4401777

Tyrrell, T., and Merico, A. (2004). "*Emiliania huxleyi*: bloom observations and the conditions that induce them," in *Coccolithophores: From Molecular Processes to Global Impact*, eds *H. R. Thierstein and J. R. Young* (Berlin: Springer), 75–97.

Von Dassow, P., John, U., Ogata, H., Probert, I., Bendif, E. M., Kegel, J. U., et al. (2015). Life-cycle modification in open oceans accounts for genome variability in a cosmopolitan phytoplankton. *ISME J.* 9, 1365–1377. doi: 10.1038/ismej.2014.221

Von Dassow, P., Ogata, H., Probert, I., Wincker, P., Da Silva, C., Audic, S., et al. (2009). Transcriptome analysis of functional differentiation between haploid and diploid cells of *Emiliania huxleyi*, a globally significant photosynthetic calcifying cell. *Genome Biol.* 10:R114. doi: 10.1186/gb-2009-10-10-r114

Von Dassow, P., Van Den Engh, G., Iglesias-Rodriguez, D., and Gittins, J. R. (2012). Calcification state of coccolithophores can be assessed by light scatter depolarization measurements with flow cytometry. *J. Plankton Res.* 34, 1011–1027. doi: 10.1093/plankt/fbs061

Wagner, N. D., Hillebrand, H., Wacker, A., and Frost, P. C. (2013). Nutritional indicators and their uses in ecology. *Ecol. Lett.* 16, 535–544. doi: 10.1111/ele.12067

Wahlund, T. M., Hadaegh, A. R., Clark, R., Nguyen, B., Fanelli, M., and Read, B. A. (2004). Analysis of expressed sequence tags from calcifying cells of marine coccolithophorid (*Emiliania huxleyi*). *Mar. Biotechnol.* 6, 278–290. doi: 10.1007/s10126-003-0035-3

Wolf-Gladrow, D. A., Zeebe, R. E., Klaas, C., Koertzinger, A., and Dickson, A. G. (2007). Total alkalinity: the explicit conservative expression and its application to biogeochemical processes. *Mar. Chem.* 106, 287–300. doi: 10.1016/j.marchem.2007.01.006

Conflict of Interest Statement: The authors declare that the research was conducted in the absence of any commercial or financial relationships that could be construed as a potential conflict of interest.